FUNDAMENTAL CHARACTERISTICS OF DECENTRALIZED AIR TRAFFIC FLOW CONTROL IN HIGH DENSITY CORRIDOR

Noboru TAKEICHI*, Yoichi NAKAMURA*,†, and Keisuke FUKUOKA*
*** Department of Aerospace Engineering, Nagoya University**
†Currently, Air Traffic Management Department, Electronic Navigation Research Institute
takeichi@nuae.nagoya-u.ac.jp; nakamura@enri.go.jp; fukuoka@nuae.nagoya-u.ac.jp

Keywords: *Air Traffic Management, Airborne Surveillance, Self-Separation, Air Corridor*

Abstract

Fundamental characteristics of decentralized separation control in a high density air corridor are discussed. A high density air corridor is expected to be an air space where aircraft capable of airborne self-separation are allowed to fly into the same direction. Some decentralized control algorithms are indispensable for its operational safety and a large traffic throughput. In this study two types of self-separation algorithms are investigated through numerical simulations: one is based on the relative velocity vector, and the other is based on the lateral position. The former algorithm is developed based on the free-flight algorithm, and the latter one is based on the assumption that all aircraft intends flying along the corridor. It is clarified that the velocity vector based algorithm leads many aircraft to perform superfluous maneuvers into lateral direction, which results in far larger conflict risk and operational inefficiency than those obtained by the lateral position based algorithm that achieved conflict free operation with high throughput throughout the all numerical simulations. It is concluded that a self-separation algorithm for a free-flight should not be directly applied for a high density air corridor operation because this algorithm cannot achieve sufficient self-separation during overtaking. Through numerical investigations it is proven that the flight intent has a significant role, and that the lateral position based algorithm has a strong capability to achieve safe and efficient operation of a self-separated high density corridor.

1 Introduction

The current oceanic routes and the cruising routes between congested airports have high density traffic, where many aircraft form a one-way high density traffic flow. Recently, it has been planned to introduce an air corridor to increase the traffic capacity and decrease the air traffic controllers' workload [1,2]. In the air corridor, aircraft will be required to be equipped with the airborne surveillance systems [3] and allowed to make the airborne separation control without air traffic controllers' instructions. Several studies have been carried out on the high density air corridor mainly concerning its design [4,5] and preliminary operation procedures [6]. However, no studies were carried out on the detail or feasibility of self-separation procedures in the air corridor prior to the authors' ones [7,8].

The airborne separation in such air corridors seems similar to the airborne in-trail separation in arrival routes [9~12]. However the in-trail separation control aims to achieve the constant interval by leading all aircraft to have the same flight speed. In contrast, the airborne separation control in the air corridor should lead all aircraft to maintain each one's optimum flight speed with keeping sufficient separation distances. The authors, therefore, have sought for an appropriate control algorithm for the high density air corridor. Generally, through trial-

and-error studies assuming some certain procedure, it is actually possible to obtain the maximum traffic capacity and a practical operation procedure to achieve it. In this case, the maximum traffic capacity is determined by the initially assumed procedure. In contrast, the authors consider that it is also possible to obtain the maximum traffic capacity that is determined by the aircraft dynamics and navigation performance, and that this traffic capacity becomes larger than the aforementioned one obtained by the procedure based study. Therefore, the authors have carried out the air corridor studies to clarify a procedure for a decentralized control that is able to operate the maximum traffic volume with sufficient safety and efficiency [7]. An appropriate route structure for the safe treatment of an air traffic with the flight speed distribution has also been proposed [8].

In this study, to find a more sophisticated and practical algorithm, the following two types of the separation control algorithms are developed and their characteristics are discussed; velocity vector based algorithm and lateral position based one. The velocity vector based algorithm is developed according to the free flight algorithm [13]. The lateral position based algorithm is based on the authors' previous studies [7,8] that refers to the aircraft lateral positions for their conflict detection and resolution. Their suitability for the self-separation in a high density air corridor are investigated through Monte-Carlo simulations.

2. Simulation Models

2. 1. Aircraft Model

The aircraft is modeled as a mass particle, and only its level motion is considered. The coordinate is shown in Fig. 1. The x and y axes are defined along the flight direction and right hand to it. The aircraft equations of motion are given as follows:

$$\dot{x}_i = v_i \cos\psi_i \tag{1}$$

$$\dot{y}_i = v_i \sin\psi_i \tag{2}$$

$$\dot{v}_i = T - D \tag{3}$$

$$\dot{\psi}_i = \frac{g}{v_i}\tan\phi_i \tag{4}$$

where v, ψ, and ϕ are the aircraft velocity, azimuth, and bank angle. i denotes the aircraft number. T and D are the thrust and drag, and g is the gravitational acceleration.

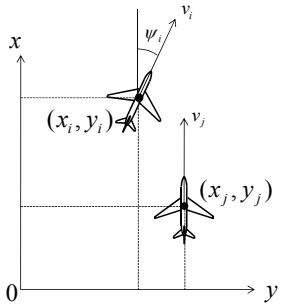

Fig. 1 Aircraft model and coordinate

2.2. Self-Separation Concept

In this study, the minimum separation distance and the separation control distance are also introduced for the conflict detection and resolution. These distances form circles around an aircraft as shown in Fig. 2, which are called the minimum separation circle and the separation control circle in this paper. Aircraft in the air corridor perform the conflict detection and resolution referring to the separation control distance in order to avoid any conflict. This concept is similar to the one presented in [14].

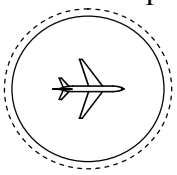

Fig. 2 Minimum separation circle (solid) and separation control circle (dashed)

2.3. Air Traffic Model

It is considered that the maximum traffic capacity would be achieved when the aircraft compose a traffic flow with the distance same as the separation control distance as shown in Fig. 3. This traffic flow is defined as the one with the maximum traffic capacity in this paper. In the following of this paper, the separation algorithms are applied to an air corridor with the traffic volume same as this traffic capacity, and

the possibility to achieve sufficient safety and efficiency is investigated.

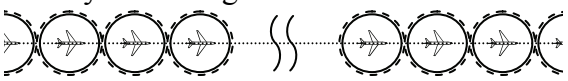

Fig. 3 Air traffic flow with maximum traffic capacity

3. Aircraft Self-Separation and Azimuth Control Algorithm

3.1. Velocity Vector based Algorithm for Self-Separation

This algorithm is developed based on a free-flight self-separation algorithm [13]. The conflict detection and resolution is carried out according to the relative velocity vector. Consider a pair of aircraft, A and B, flying on the same level with velocity vectors $\mathbf{V}_A$ and $\mathbf{V}_B$ at the position $\mathbf{P}_A$ and $\mathbf{P}_B$ as depicted in Fig. 4. The conflict is detected if the relative velocity vector $\mathbf{V}_R$ is expected to fly into the separation control circle. This is evaluated through the following equation:

$$|\alpha| < \beta \tag{5}$$

where α is the direction angle of the relative velocity measured from the relative position vector, and β is the width angle of the separation control distance measured from the aircraft A. α and β are given as follows:

$$\cos\alpha = \frac{(\mathbf{P}_B - \mathbf{P}_A)\cdot(\mathbf{V}_A - \mathbf{V}_B)}{\|\mathbf{P}_B - \mathbf{P}_A\|\|\mathbf{V}_A - \mathbf{V}_B\|} \tag{6}$$

$$\sin\beta = \frac{R_{SC}}{d_{A,B}} \tag{7}$$

where R_{SC} and $d_{A,B}$ are the separation control distance and the distance between the aircraft A and B.

To achieve the conflict resolution, the direction angle of the relative velocity vector should be changed by $\gamma \equiv \beta - \alpha$. In this paper it is supposed that both aircraft simultaneously change its azimuth angle by μ_{sc} into the opposite direction as shown in Fig. 5. The relative velocity after azimuth change is given as:

$$\mathbf{V}'_R = \begin{pmatrix} V_A\cos(\psi_A - \mu_{sc}) - V_B\cos(\psi_B + \mu_{sc}) \\ V_A\sin(\psi_A - \mu_{sc}) - V_B\sin(\psi_B + \mu_{sc}) \end{pmatrix} \tag{8}$$

where $V_A = \|\mathbf{V}_A\|$, $V_B = \|\mathbf{V}_B\|$, and azimuth angle of the aircraft A and B are denoted by ψ_A and ψ_B. This vector should be parallel to the one that is rotated by γ from the original relative velocity vector $\mathbf{V}_R$. This is described as:

$$\mathbf{V}'_R \parallel \begin{pmatrix} V_A\cos(\psi_A - \gamma) - V_B\cos(\psi_B - \gamma) \\ V_A\sin(\psi_A - \gamma) - V_B\sin(\psi_B - \gamma) \end{pmatrix} \tag{9}$$

The maneuver angle μ_{sc} is obtained as the following equation to achieve the necessary rotation of the relative velocity vector:

$$\tan\mu_{sc} = \frac{\left(V_A^2 + V_B^2 - 2V_AV_B\cos(\psi_A - \psi_B)\right)\sin\gamma}{\left(V_A^2 - V_B^2\right)\cos\gamma + 2V_AV_B\sin\gamma\sin(\psi_A - \psi_B)} \tag{10}$$

In case the distance between aircraft becomes smaller than the separation control distance, some maneuver to avoid conflict should be made in addition to the conflict resolution maneuver. In this study, an azimuth change angle proportional to the distance below the separation control distance is given into the same direction as μ_{sc} as follows:

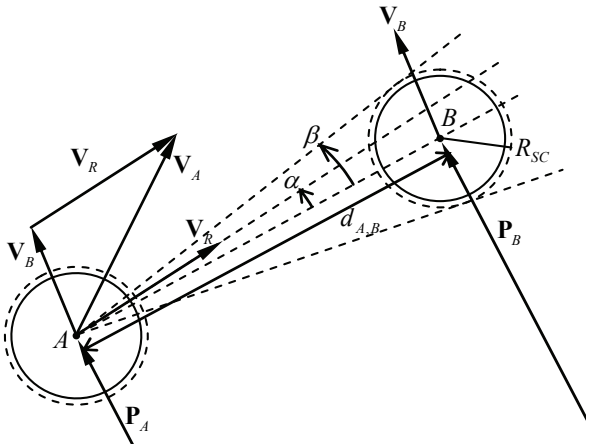

Fig. 4 Velocity vector based algorithm

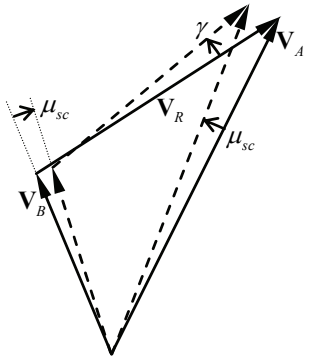

Fig. 5 Maneuver for conflict resolution in velocity vector based algorithm

$$\mu_a = \frac{R_{SC} - d_{A,B}}{R_{SC} - R_{MS}} \frac{\pi}{2} \tag{11}$$

where R_{MS} denotes the minimum separation distance. When the distance reduces to be near the minimum separation distance, the given azimuth change angle becomes near 90 degrees to achieve swift separation maneuver.

An urgent maneuver is also introduced to recover the aircraft distance in case of the conflict. When the aircraft distance becomes smaller than the minimum separation distance, the following azimuth angle is given into the opposite direction to the other aircraft:

$$\mu_u = \frac{\pi}{2} \tag{12}$$

The azimuth change for the separation control is summarized as follows:

$$\mu_{A,B} = \begin{cases} \mu_{sc} & \left(d_{A,B} > R_{SC}\right) \\ \mu_{sc} + \mu_a & \left(R_{SC} \geq d_{A,B} > R_{MS}\right) \\ \mu_u & \left(R_{MS} \geq d_{A,B}\right) \end{cases} \tag{13}$$

3.2. Lateral Position based Algorithm for Self-Separation

Because all aircraft intend to fly into the same direction in the corridor, it is expected possible to achieve safe self-separation based on the lateral position. Consider the aircraft A overtaking another aircraft B shown in Fig. 6. The conflict is detected if the aircraft A is flying faster than the aircraft B and its lateral position is within the lateral separation control circle width of the aircraft B. To avoid conflict, in the same way as the velocity vector based algorithm, it is supposed that both aircraft make azimuth change maneuver into opposite direction by μ_{sc} as shown in Fig. 7. To achieve the conflict resolution with the minimum azimuth change, the relative velocity vector should be directed toward the tangential line of the separation control circle as shown in Fig. 6.

The condition that the relative velocity rotates by γ to be tangential to the separation control circle is given as:

$$R_{SC} = d^x_{A,B} \sin\gamma + d^y_{A,B} \cos\gamma \tag{14}$$

where $d^x_{A,B}$ and $d^y_{A,B}$ are the distances between these aircraft along x and y axes. The azimuth change angle μ_{sc} should satisfy the following equation:

$$\frac{R_{SC}\cos\gamma - d^y_{A,B}}{\left(V_A + V_B\right)\sin\mu_{sc}} = \frac{d^x_{A,B} - R_{SC}\sin\gamma}{\left(V_A - V_B\right)\cos\mu_{sc}} \tag{15}$$

This equation means the necessary time for the aircraft A to reach the separation control circle of the aircraft B along the tangential line. The left hand is the lateral distance divided by the lateral relative velocity, and the right hand is the longitudinal one. From the above equations the azimuth change angle μ_{sc} is obtained as follows:

$$\tan\mu_{sc} = \frac{\left(R_{SC}\cos\gamma - d^y_{A,B}\right)\left(V_A - V_B\right)}{\left(-R_{SC}\sin\gamma + d^x_{A,B}\right)\left(V_A + V_B\right)} \tag{16}$$

Likewise the velocity vector based algorithm, when the distance between aircraft becomes smaller the separation control distance, the following azimuth change is given in addition to μ_{sc} for the swift conflict avoidance

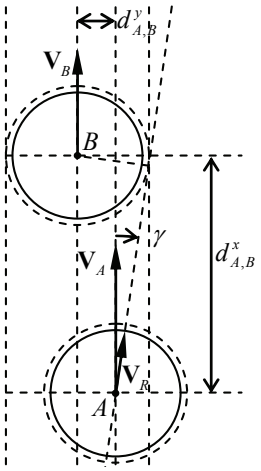

Fig. 6 Lateral position based algorithm

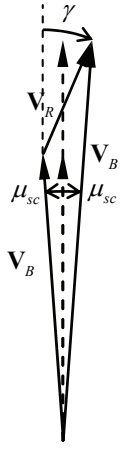

Fig. 7 Maneuver for conflict resolution in lateral position based algorithm

maneuver:

$$\mu_a = \frac{R_{SC} - d_{A,B}}{R_{SC} - R_{MS}} \frac{\pi}{2} \tag{17}$$

The same urgent maneuver as the velocity vector based algorithm is also introduced:

$$\mu_u = \frac{\pi}{2} \tag{18}$$

The azimuth change for the separation control is summarized as follows:

$$\mu_{A,B} = \begin{cases} \mu_{sc} & \left(d_{A,B} > R_{SC}\right) \\ \mu_{sc} + \mu_a & \left(R_{SC} \geq d_{A,B} > R_{MS}\right) \\ \mu_u & \left(R_{MS} \geq d_{A,B}\right) \end{cases} \tag{19}$$

3.3. Aircraft Azimuth Control Algorithm [7,8]

The aircraft azimuth angle is controlled through the bank angle. The bank angle is given according to:

$$\phi_i = a\left(\Psi_i - \psi_i\right) \tag{20}$$

where a is a positive coefficient, and Ψ_i is the target azimuth angle of the i th aircraft. Ψ_i is given as follows:

$$\Psi_i = \psi_r\left(y_i\right) + \sum_{j \neq i} \mu_{i,j} \tag{21}$$

The target azimuth angle Ψ_i is determined so as to lead the i th aircraft to achieve separation control with plural aircraft, and to turn back to the corridor when it is flying its outside. The bank angle is given proportional to the difference between the azimuth angle ψ_i and the target one Ψ_i . The function $\psi_r\left(y_i\right)$ is defined as follows:

$$\psi_r\left(y_i\right) = \begin{cases} -b\left(y_i - y_{edge}^{+}\right) & \left(y_i > y_{edge}^{+}\right) \\ 0 & \left(y_{edge}^{-} < y_i < y_{edge}^{+}\right) \\ -b\left(y_i - y_{edge}^{-}\right) & \left(y_i < y_{edge}^{-}\right) \end{cases} \tag{22}$$

where y_{edge}^{+} and y_{edge}^{-} are the y positions of the corridor edges. In order to enable all the aircraft to fly on each ones' optimum flight speed, no deceleration or acceleration are considered in the separation control, and $T = D$ and $\dot{v}_i = 0$.

4. Numerical Analyses

4.1. Parameters and Assumptions

In the numerical simulations, the minimum separation distance R_{MS} and the separation control distance R_{SC} are set 10NM (=18520m) and 10.5NM (=19446m), respectively. It is assumed that the conflict detection and resolution are carried out against aircraft within 50NM. The air traffic flow is composed of 20 aircraft. The aircraft are placed along x axis with intervals equal to the separation control distance, and placed randomly along y axis for the initial condition as shown in Fig. 8. The analysis range is fixed, and the front of this range is considered linking to the end to simulate an infinite length traffic flow. When an aircraft's separation control distance exceeds the front of the analysis range, the aircraft takes the aircraft around the end of the analysis range into account for its separation control, and vice versa. The each aircraft flight speed is given randomly according to the uniform distribution between 230m/s and 250m/s. The corridor width is given as 3 times of the separation control distance. The analysis range and the corridor width are also shown in Fig. 8. In this figure, the circles surrounding each aircraft denote the minimum separation circles, and the arrows exaggeratingly denote the flight speed and direction, where the aircraft azimuth angles are exaggerated 5 times. The colors of the minimum separation circles show the aircraft flight speed according to the color bar. The air traffic behavior converges to some steady state flow as the simulation time progresses. To focus on the traffic behavior difference due to the separation control strategy, long term simulations are necessary, and all numerical simulations are

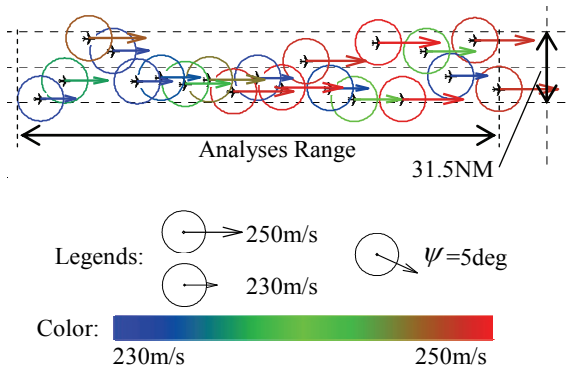

Fig. 8 Initial condition and analysis range

carried out for 100000sec. Table 1 shows the simulation parameters. Numerical simulations are carried out using 50 sets of initial conditions.

Table 1 Simulation parameters

No. of Aircraft	20
Speed Range	230~250[m/s]
Separation Control Distance	10.5[NM]
Minimum Separation Distance	10.0[NM]
Corridor Width	31.5[NM]
a	1.0
b	1.0[rad/km]

4.2. Evaluation Indices [7,8]

The following indices are applied to evaluate the air traffic safety and pilots' workload. All aircraft are required to have distances larger than the minimum separation distance to avoid conflict, and it is also more desirable that the distances are larger than the separation control distance. To evaluate the safety, $d_{i,j}^{conf}$ and $d_{i,j}^{ctrl}$ are introduced as following equations:

$$d_{i,j}^{conf} = \begin{cases} 10NM - d_{i,j} & \left(d_{i,j} < 10NM\right) \\ 0 & \left(d_{i,j} \geq 10NM\right) \end{cases}$$
$$d_{i,j}^{ctrl} = \begin{cases} 10.5NM - d_{i,j} & \left(d_{i,j} < 10.5NM\right) \\ 0 & \left(d_{i,j} \geq 10.5NM\right) \end{cases} \quad (23)$$

, and the evaluation indices accounting for safety E_{conf} and E_{ctrl} are introduced as follows:

$$E_{conf} = \frac{1}{N}\sum_{i,j}\int d_{i,j}^{conf}\,dt \quad (i<j)$$
$$E_{ctrl} = \frac{1}{N}\sum_{i,j}\int d_{i,j}^{ctrl}\,dt \quad (i<j) \quad (24)$$

, where N is the number of aircraft. E_{conf} and E_{ctrl} are defined as the average of the time integration of the aircraft distances below the minimum separation distance and the separation control distance, respectively. Because the conflict between aircraft must be avoided for safety assurance, $E_{conf} = 0$ are mandatory throughout numerical simulations. In addition, it is desirable that E_{ctrl} has a smaller value so as to minimize the conflict possibility.

It is also desirable for the feasibility of the separation control algorithm that the pilots' workload is smaller as possible. In this paper the workload is considered proportional to the amount of the azimuth angle change, and the index E_{work} is defined as follows:

$$E_{work} = \frac{1}{N}\sum_{i}\int |\dot{\psi}_i|dt \quad (25)$$

To eliminate the influence of the initial conditions as possible, the evaluation indices are calculated after 20000sec.

4. 3. Numerical Simulation and Evaluation

4.3.1. Velocity Vector Based Algorithm

Fig. 9 shows the basic conflict resolution maneuver. The aircraft A is flying at 250m/s at the center of the corridor overtaking another aircraft B flying at 230m/s at 5NM right and 40NM ahead. In this case, the aircraft A and B begin turning into left and right, respectively, to achieve the required separation cooperatively. The conflict resolution is achieved in a different manner when the aircraft have azimuth angles. In Fig. 10, the aircraft B is initially heading left by 0.05rad. In this case these aircraft begin turning into the opposite direction to achieve conflict resolution with the smaller azimuth change.

The example illustration of the 20 aircraft traffic simulation result using the initial condition shown in Fig. 8 is presented in Fig. 11, where the aircraft positions, velocity, and azimuth angles are depicted every 25000sec. The yellow shadow means that the distance between the shadowed aircraft and one of its surrounding aircraft is below the separation control distance. If the distance between aircraft becomes smaller than the minimum separation distance, the aircraft will be depicted with red shadow. As a result, the conflict occurred in 32 cases out of 50. The typical conflict situation is depicted in Fig. 12, where the azimuth angles are shown with no exaggeration. The conflict occurs between the aircraft A, B, and C. The conflict resolution maneuver between the aircraft B and D is the trigger of the conflict. In Fig. 12a, although D aircraft is about to overtake the aircraft B and C, the separation distances between them are insufficient. This leads the aircraft B and D to get close below the separation control distance as shown in Fig. 12b, and they make swift turning for conflict

resolution. However, a large azimuth change of the aircraft D involves the aircraft A and C to make large azimuth changes as shown in Fig. 12c. The aircraft C turns left for the conflict resolution between the aircraft D, and this leads the aircraft A to turn right to resolve the conflict with the aircraft C. Such fast maneuvers into lateral direction result in the conflict as shown in Fig. 12d. Even in this situation the urgent maneuver resolves conflict soon as shown in Fig. 12e.

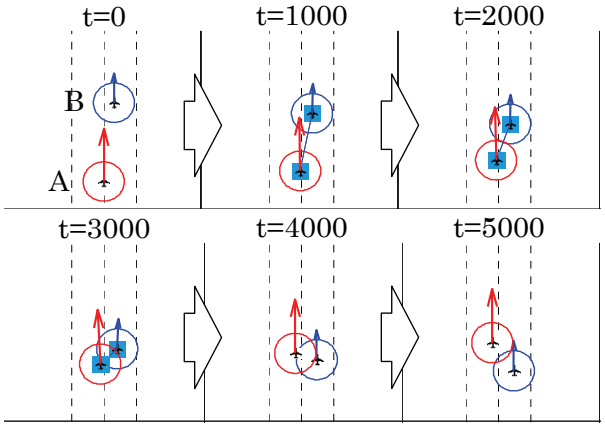

Fig. 9 Basic conflict resolution maneuver, velocity vector based algorithm

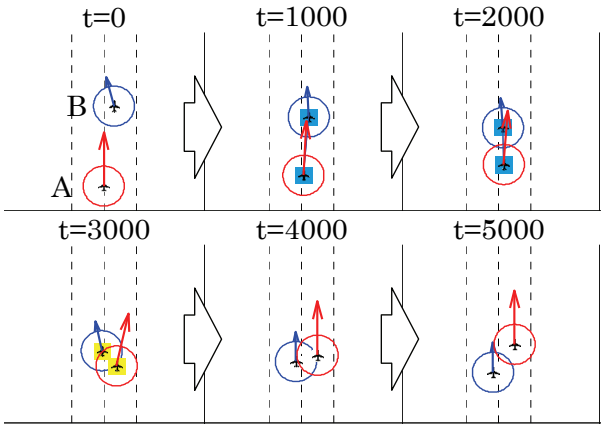

Fig. 10 Basic conflict resolution maneuver, velocity vector based algorithm (initial azimuth angle case)

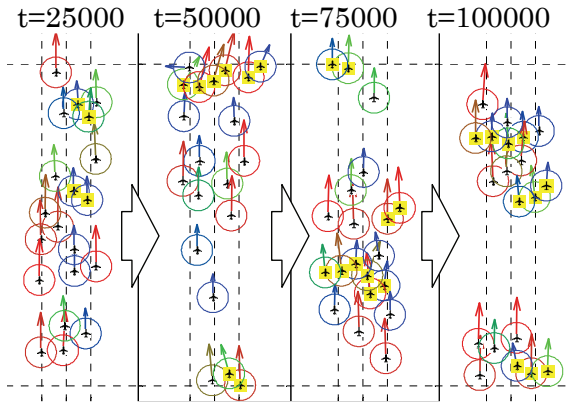

Fig. 11 Example behavior in traffic simulation, velocity vector based algorithm

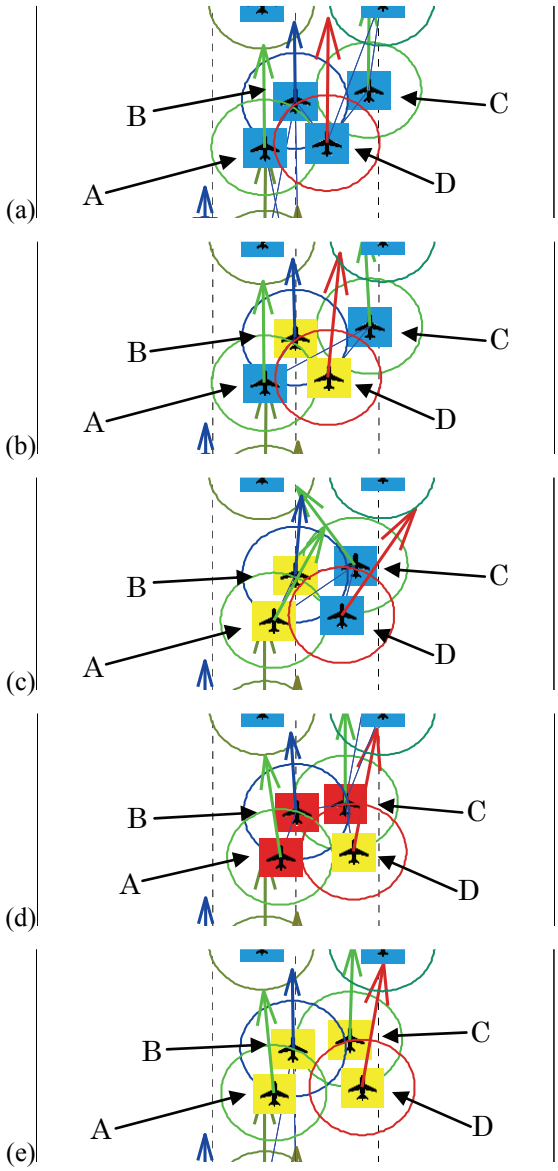

Fig. 12 Typical conflict situation, velocity vector based algorithm (no azimuth exaggeration)

4.3.2. Lateral Position Based Algorithm

A basic conflict resolution maneuver is shown in Fig .13. The initial conditions are same as those used in Fig. 9 case. Both aircraft behaves in almost the same manner as the velocity vector based algorithm case. However, both aircraft turn into the same direction even when the aircraft initially has the azimuth angle as shown in Fig. 14 because the lateral position based algorithm does not refer to the aircraft azimuth.

The aircraft behavior in the traffic simulation using the initial condition shown in Fig. 8 is shown in Fig. 15. It is found that the aircraft do not make so large azimuth change as those in the velocity vector based algorithm case. It is noteworthy that no conflict occurred throughout the 50 simulation cases.

The evaluation indices are summarized in Table 2. All evaluation indices have considerably decreased in the lateral position based algorithm case. The lateral position based algorithm is based on an assumption that every aircraft intends flying along the corridor, and the aircraft azimuth angles are not considered in the conflict detection and resolution. Therefore the algorithm enables aircraft in the corridor to perform the minimum conflict detection and resolution for the safe and efficient operation.

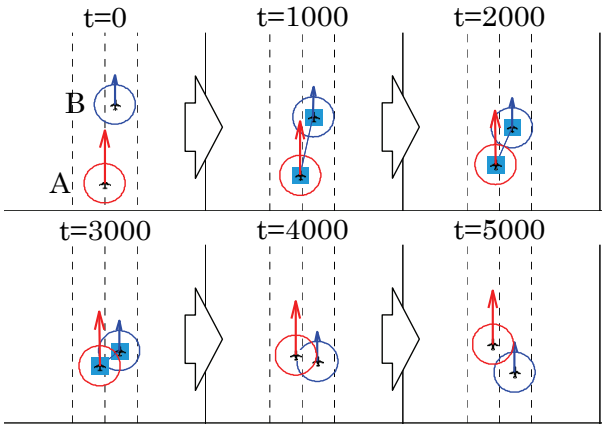

Fig. 13 Basic conflict resolution maneuver, lateral position based algorithm

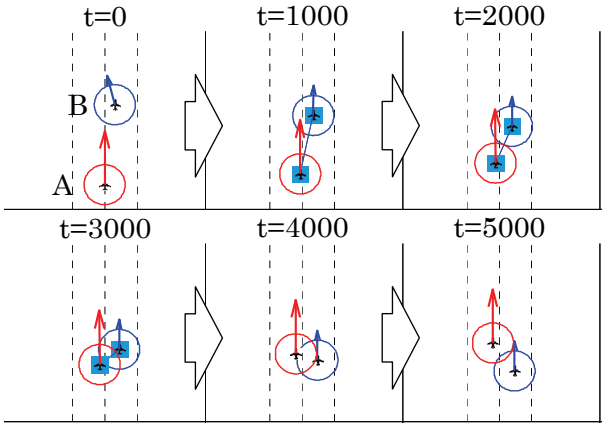

Fig. 14 Basic conflict resolution maneuver, lateral position based algorithm (initial azimuth angle case)

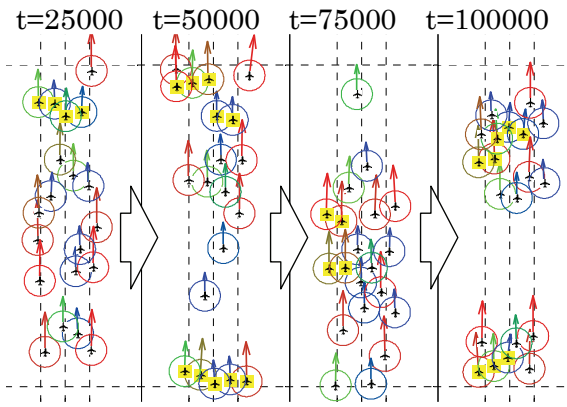

Fig. 15 Example behavior in traffic simulation, lateral position based algorithm

Table 2 Evaluation indices summary

	E_{ctrl}	E_{conf}	E_{work}
Velocity Vector Based	7.9×10^{5}	5.9×10^{2}	6.4
Lateral Position Based	9.7×10^{4}	0	1.1

5. Conclusion

The fundamental behavior of the decentralized air traffic flow control in a high density air corridor is investigated through numerical simulations. It has been clarified that a typical self-separation algorithm for a free-flight should not be directly applied for the self-separation in a high density corridor. It is also demonstrated that a self-separation algorithm using corridor flight intent achieves the conflict free operation with a large traffic throughput.

There are a lot of future works to bring the self-separated high density corridor into practical use, e.g. three-dimensional maneuver for conflict avoidance, dynamic configuration change of corridors, etc. In addition to the flight speed distribution, it is also expected that the swiftness of the conflict avoidance maneuver and the condition to begin it will have some distribution due to the aircraft types, weight etc. Investigations on emergency procedures are also indispensable. It is also an important subject to find simplified separation control strategies so that the human pilots are actually able to make appropriate maneuvers for conflict resolution. The evaluation indices must also be improved so that they can evaluate the self-separation procedure from a more practical viewpoint.

References

[1] Japan Civil Aviation Bureau. Long-term Vision for the

Future Air Traffic Systems (CARATS), 2010, http://www.mlit.go.jp/koku/koku_CARATS.html, cited Jun. 29, 2012.
[2] Joint Planning and Development Office. Concept of Operation for the Next Generation Air Transportation System Ver.3.2., Sep. 30, 2010, http://jpe.jpdo.gov/ee/docs/conops/NextGen_ConOps_v3_2.pdf, cited Jun. 29, 2012.
[3] FAA/Eurocontrol Cooperative R&D Committee. Principles of Operation for the Use of Airborne Separation Assurance Systems version: 7.1, 2001, http://adsb.tc.faa.gov/RFG/po-asas71.pdf, cited Jun. 29, 2012.
[4] Yousefi, A., et al. Dynamic Allocation and Benefit Assessment of NextGen Flow Corridors. *10th AIAA ATIO Conference*, Fort Worth, Texas, 2010.
[5] Xue, M. Design Analysis of Corridors-in-the-sky. AIAA 2009-5859, *AIAA Guidance, Navigation, and Control Conference*, Chicago, Aug. 10-13, 2009.
[6] Yousefi, A., Lard, J., and Timmerman, J. Nextgen Flow Corridors Initial Design, Procedures, and Display Functionalities. *IEEE/AIAA 29th Digital Avionics Systems Conference*, Oct. 3-7, 2010.
[7] Nakamura, Y. and Takeichi, N. Unidirectional Air Traffic Flow Control Using Airborne Surveillance. *Journal of the Japan Society for Aeronautical and Space Sciences*, Vol. 59, 2011, pp.76-82. (in Japanese)
[8] Nakamura, Y. and Takeichi, N. Decentralized Control of an Unidirectional Air Traffic Flow with Flight Speed Distribution. *Journal of the Japan Society for Aeronautical and Space Sciences*, Vol. 60, 2012, pp.17-23. (in Japanese)
[9] Abbott, T.S. Speed control law for precision terminal area in-trail self spacing. *NASA TM-2002-211742*, 2002.
[10] Ivanescu, D., Shaw, C., Zeghal, K., and Hoffman, E. Propagation of airborne spacing errors in merging traffic streams. *Proceedings of the 7th USA/Europe Air Traffic Management R&D Seminar*, Barcelona, Spain, Jul. 2007.
[11] Barmore, B.E., Abbott, T.S., Capron, W.R., Baxley, B.T. Simulation results for airborne precision spacing along continuous descent arrivals. *Proceedings of the AIAA Aviation Technology, Integration, and Operations Conference*, 2008.
[12] Weitz, L.A. Investigating string stability of a time-history control law for Interval Management. *Transportation Research Part C: Emerging Technologies*, in press, available on line: http://dx.doi.org/10.1016/j.trc.2011.10.002
[13] Bach R., Farrell C., and Erzberger H. An algorithm for level-aircraft conflict resolution. *NASA/CR-2009-214573*, 2009.
[14] Cuevas, G., Echegoyen, I., Garc´ıa, J., C´asek, P., Keinrath, C., Bussink, F., and Luuk A. Autonomous Aircraft Advanced (A3) ConOps. *iFly Project, Technical Report* Deliverable D1.3, 2008.

Copyright Statement